Analysis of Baryon Transition Electromagnetic Form Factors

Teresa Peña
in collaboration with
Gilberto Ramalho

TÉCNICO LISBOA
LIP
OMEG
Origin of Matter and Evolution of Galaxies
우주 물질 중점연구소
DF
DEPARTAMENTO DE FÍSICA
TÉCNICO LISBOA
DECN
DEPARTAMENTO DE ENGENHARIA E CIÊNCIAS NUCLEARES
TÉCNICO LISBOA

- Hadrons constitute the major part of the visible universe.

- Today's experiments have a new level of scope, precision and accuracy on the still unexplored territory of Hadron structures

(evidence for multiquark and exotic configurations.)

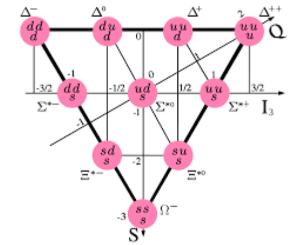

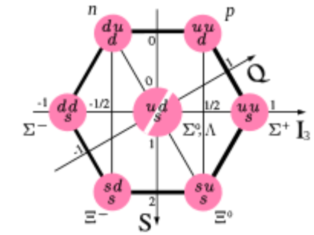

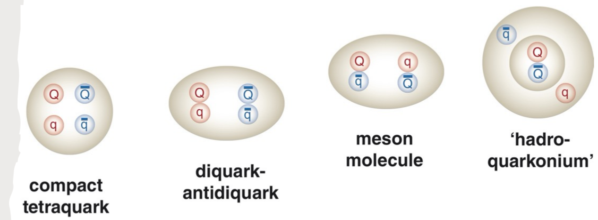

Special role of HADES@SIS at GSI and PANDA at FAIR:

- Exploring QCD phase diagram at high baryonic number and moderate temperatures

- Experiments with pion beam also allow for cold matter studies in the few-GeV region.

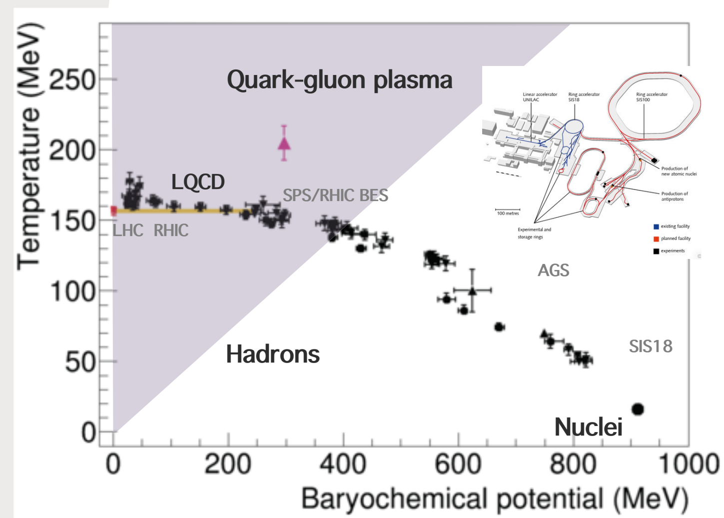

Two methods of obtaining information on structure of baryons

Figure: B. Ramstein, AIP Conf. Proc. 1735, 080001 (2016) [HADES]

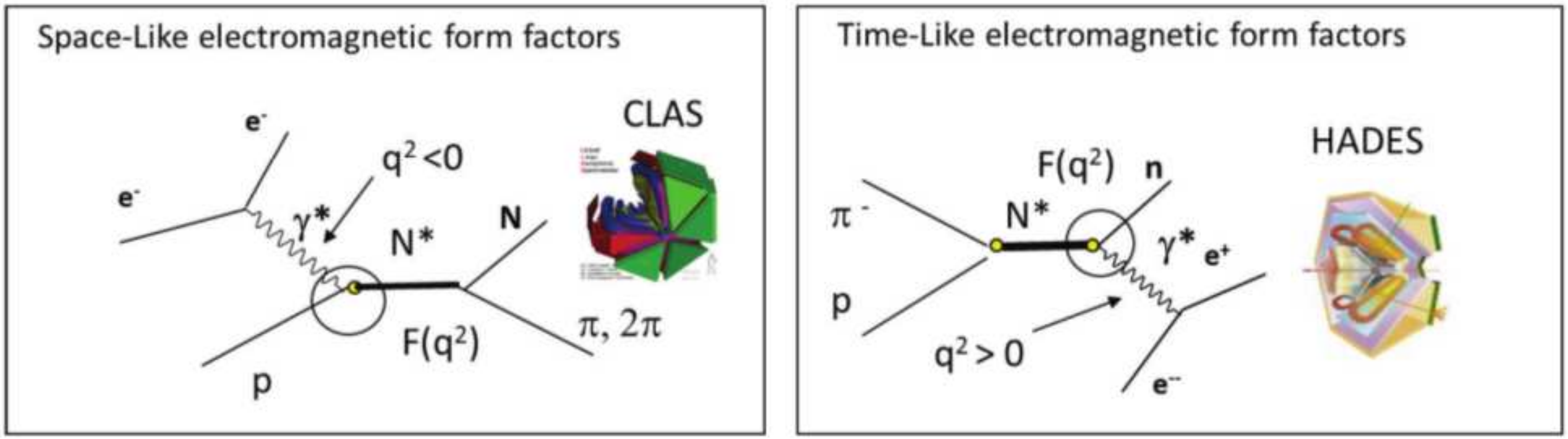

$q^2 \leq 0$: CLAS/Jefferson Lab, MAMI, ELSA, JLab-Hall A, MIT-BATES

$ep \to e'N(\cdots)$; $\gamma^* N \to N^*$

$q^2 > 0$: HADES, ..., PANDA

$\pi^- p \to e^+ e^- n$; $N^* \to \gamma^* N \to e^+ e^- N$

Why use of pion beam :
Separation of in-medium propagation and mechanism, because pions are absorbed at the surface of the nucleus whereas in photon and proton absorption occurs throughout the whole nuclear volume.

Transition Electromagnetic form factors

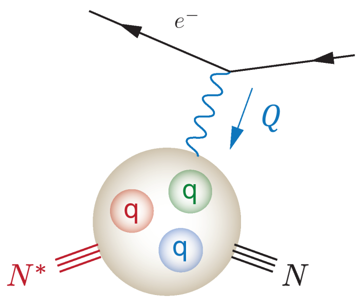

Baryon resonances
transition form factors

CLAS: Aznauryan et al., Phys. Rev. C 80 (2009)

MAID: Drechsel, Kamalov, Tiator, EPJ A 34 (2009)

See Gernot Eichmann and Gilberto Ramalho
Phys. Rev. D 98, 093007 (2018)

$q^2<0$

Spacelike form factors:

- Structure information: shape, qqq excitation vs. hybrid, ...

$q^2>0$

Timelike form factors:

- Particle production channels

This talk:
Connect Timelike and SpacelikeTransition Form Factors (TFF)
Obtain Baryon-photon coupling evolution with 4 momentum transfer

Baryon resonances S=0 PDG

I	S	$J^P = \frac{1}{2}^+$	$\frac{3}{2}^+$	$\frac{5}{2}^+$	$\frac{1}{2}^-$	$\frac{3}{2}^-$	$\frac{5}{2}^-$
$\frac{1}{2}$	0	**N(940)** **N(1440)** $N(1710)$ $N(1880)$	**N(1720)** $N(1900)$	**N(1680)** $N(1860)$	**N(1535)** **N(1650)** $N(1895)$	**N(1520)** $N(1700)$ $N(1875)$	**N(1675)**
$\frac{3}{2}$	0	**Δ(1910)**	**Δ(1232)** $\Delta(1600)$ $\Delta(1920)$	**Δ(1905)**	**Δ(1620)** $\Delta(1900)$	**Δ(1700)** $\Delta(1940)$	$\Delta(1930)$

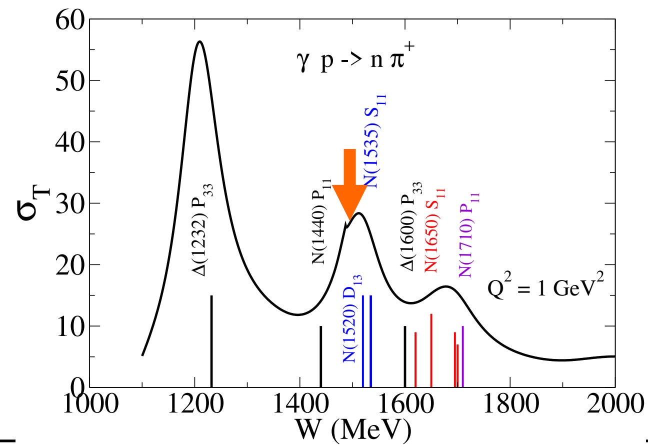

Our approach is phenomenological

“Murray looked at two pieces of paper, looked at me and said
‘***In our field it is costumary to put theory and experiment on the same piece of paper***’.
I was mortified but the lesson was valuable”

Memories of Murray and the Quark Model
George Zweig, Int.J.Mod.Phys.A25:3863-3877,2010

Zweig quark or the constituent quark

E.M. matrix element

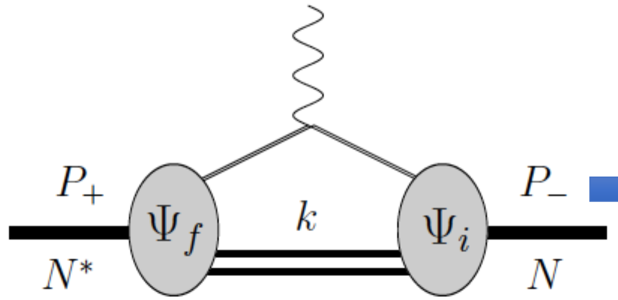

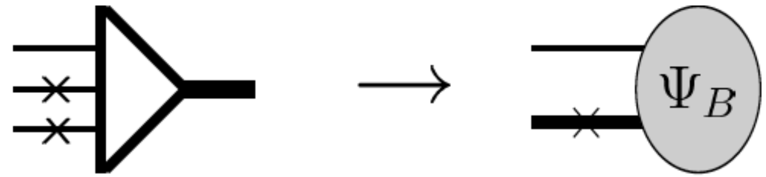

$$\int_{k_1k_2} \equiv \int \frac{d^4k_1 d^4k_2}{(2\pi)^6}\delta_+(m_1^2-k_1^2)\delta_+(m_2^2-k_2^2)$$
$$= \int \frac{d^3k_1 d^3k_2}{(2\pi)^6 4E_1E_2},$$

$$\int_{sk} = \underbrace{\int \frac{d\Omega_{\hat{\mathbf{r}}}}{4(2\pi)^3}\int_{4m_q^2}^{\infty} ds\sqrt{\frac{s-4m_q^2}{s}}}_{\int_s}\underbrace{\int \frac{d^3k}{(2\pi)^3 2E_s}}_{\int_k},$$

- **Baryon wavefunction integrated over** spectator quarks variables.
(Covariant Spectator Model CST)

- **E.M.** matrix element is then written in terms of
an effective vertex composed by an off-mass-shell quark,
and an on-mass-shell quark pair (diquark) with an average mass.

✓ The Diquark is not pointlike.

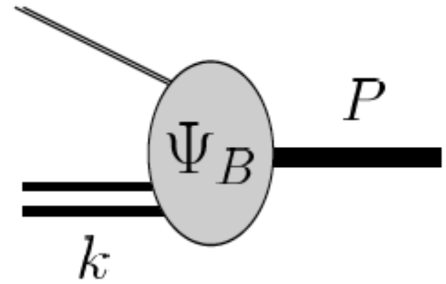

- Nucleon "wavefunction" (S wave)

(symmetry based only; not dynamical based)

- A quark + **scalar**-diquark component
- A quark+ **axial vector**-diquark component

$$\Psi^S_{N\lambda_n}(P,k) = \frac{1}{\sqrt{2}}[\phi^0_I u_N(P,\lambda_n) - \phi^1_I \varepsilon^{\alpha *}_{\lambda P} U_\alpha(P,\lambda_n)] \times \psi^S_N(P,k).$$

→ Phenomenological function

$$U_\alpha(P,\lambda_n) = \frac{1}{\sqrt{3}}\gamma_5\left(\gamma_\alpha - \frac{P_\alpha}{m_H}\right)u_N(P,\lambda_n),$$

- Delta (1232) "wavefunction" (S wave)
  - Only quark + **axial vector**-diquark term contributes

$$\Psi^S_\Delta(P,k) = -\psi^S_\Delta(P,k)\tilde{\phi}^1_I \varepsilon^{\beta *}_{\lambda P} w_\beta(P,\lambda_\Delta)$$

Quark E.M. Current

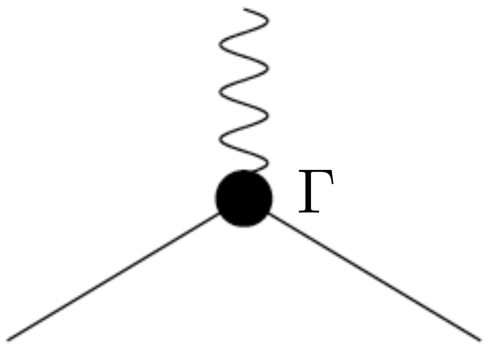

quark-antiquark
⊕ gluon dressing

Quark-photon vertex

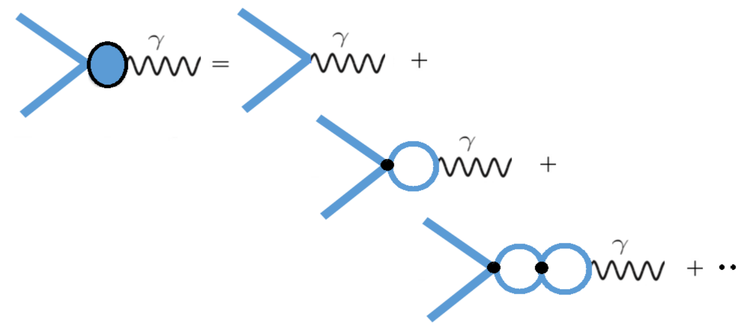

$$\Gamma_\mu(p,Q) = \gamma_\mu + \int \frac{d^4q}{(2\pi)^4} K(p,q,Q) S(q+\eta Q) \Gamma_\mu(q,Q) S(q-\eta Q)$$

Constituent quarks (quark form factors)

$$j_I^\mu = \left[\frac{1}{6} f_{1+} + \frac{1}{2} f_{1-} \tau_3\right] \gamma^\mu + \left[\frac{1}{6} f_{2+} + \frac{1}{2} f_{2-} \tau_3\right] \frac{i\sigma^{\mu\nu} q_\nu}{2M_N}$$

To parametrize the current we use Vector Meson Dominance at the quark level, a truncation to the rho and omega poles of the full meson spectrum contribution to the quark-photon coupling.

4 parameters

Transition E.M. Current

$$\gamma N \to \Delta$$

$$\Gamma^{\beta\mu}(P,q) = \left[G_1 q^\beta \gamma^\mu + G_2 q^\beta P^\mu + G_3 q^\beta q^\mu - G_4 g^{\beta\mu} \right] \gamma_5$$

- Only 3 G_i are independent:
  E.M. Current has to be conserved

$$q^\mu \Gamma_{\beta\mu} = 0 \quad \Rightarrow$$

G_M, G_E, G_C Scadron-Jones popular choice.

Model independent feature (Covariant Spectator Theory)

$$\gamma N \rightarrow \Delta \qquad \qquad G_M^* = G_M^B + G_M^\pi$$

Separation seems to be supported by experiment.
Missing strength of G_M at the origin.

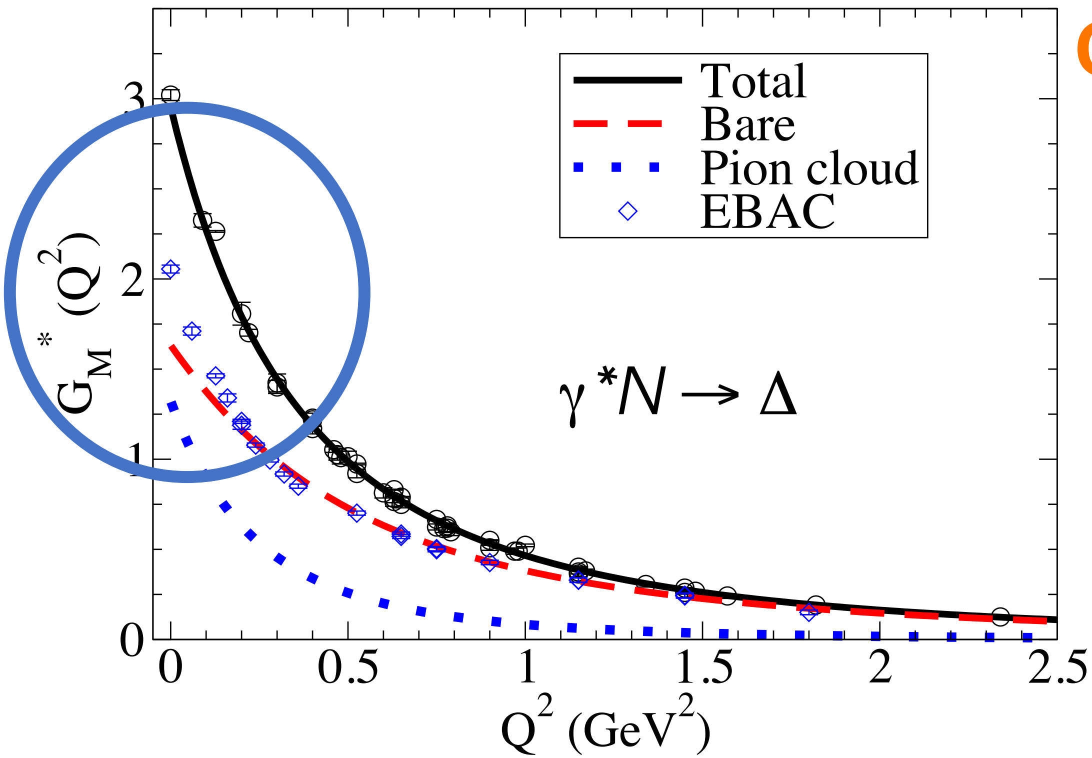

CST© 2009

Bare quark core:

- dominates in the large Q^2 region.
- agrees with other calculations ("EBAC") with pion couplings switched off.

Model independent feature

$$\gamma N \to \Delta$$

Missing strength of G_M at the origin is an universal feature, even in dynamical quark calculations.

Eichmann et al., Prog. Part. Nucl. Phys. 91 (2016)

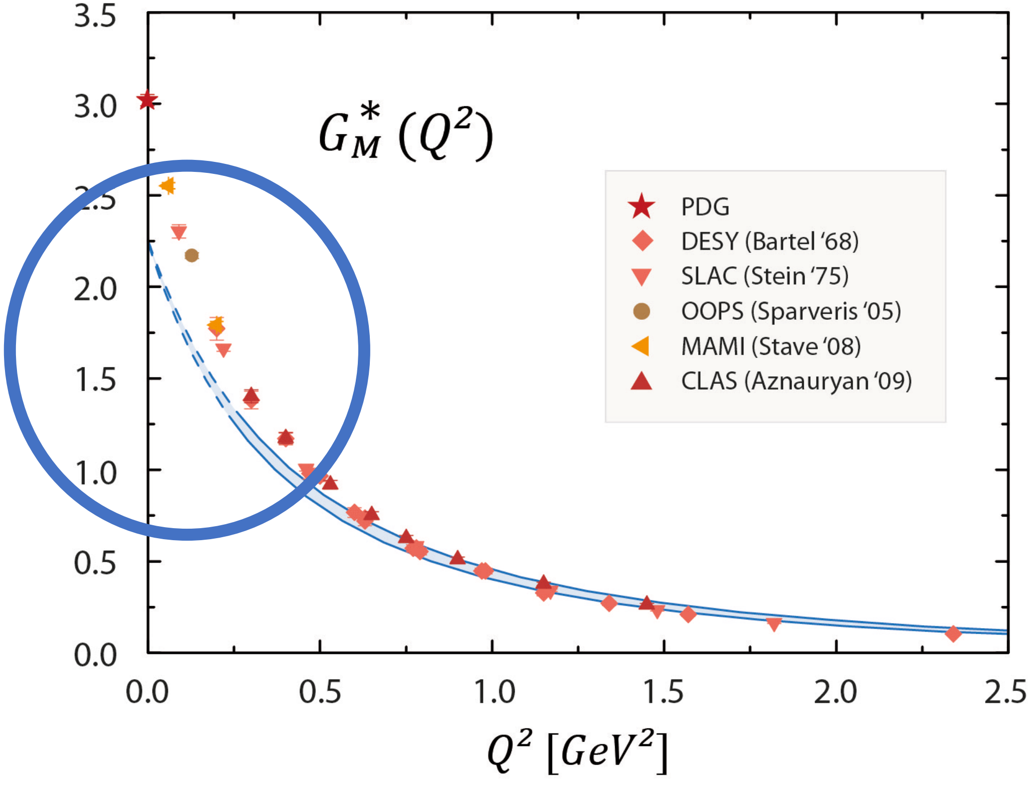

Effect of vicinity of the mass of the Delta to the pion-nucleon threshold.

$$G_M^* = G_M^B + G_M^\pi$$

Bare quark (partonic) and pion cloud (hadronic) components

For low Q^2 : add coupling with pion in flight.

Bare quark component

Pion cloud component

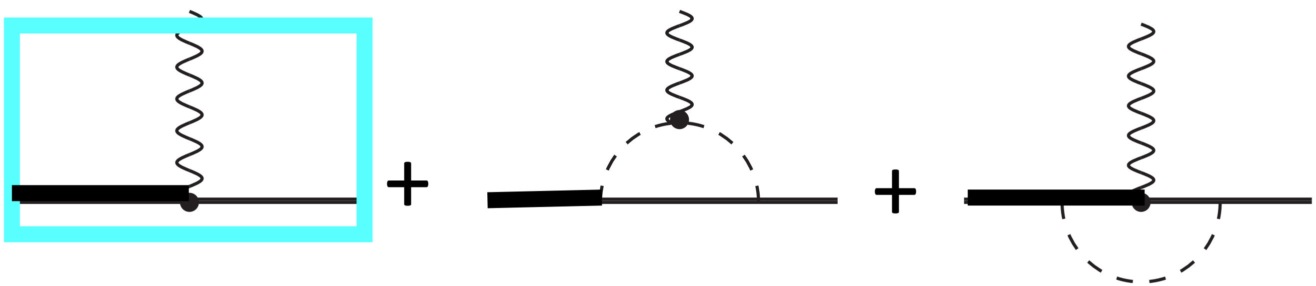

$q\bar{q}$ pairs from a single quark included in dressing

Pion created by the overall baryon not from a single quark

Pion cloud component suppressed for high Q^2 $\frac{1}{Q^8}$

VMD as link to LQCD

experimental data
well described in
the large Q^2 region.

VMD

In the current the **vector meson** mass is taken as a function of the running pion mass.

Pion cloud contribution negligible for **large pion masses**

quark model
calibrated to the
lattice data

Take the limit of the physical pion mass value

$N \rightarrow N^*(1520)$ TFFs

$J^P=3/2^-$ I=1/2
60% decay πN
30% decay to $\pi\Delta$

- Bare quark model gives good description in the high momentum transfer region.
- Use CST quark model to infer meson cloud from the data.
- Important role of meson cloud extracted dominated by the isovector part, due to the πN and $\pi\Delta$ channels.

Consistent with Aznauryan and Burkert, PRC 85 055202 2012 and PDG

$$A^V_{3/2} \approx 0.13 \; ; A^S_{3/2} \approx 0.01 \; (GeV^{-1/2})$$

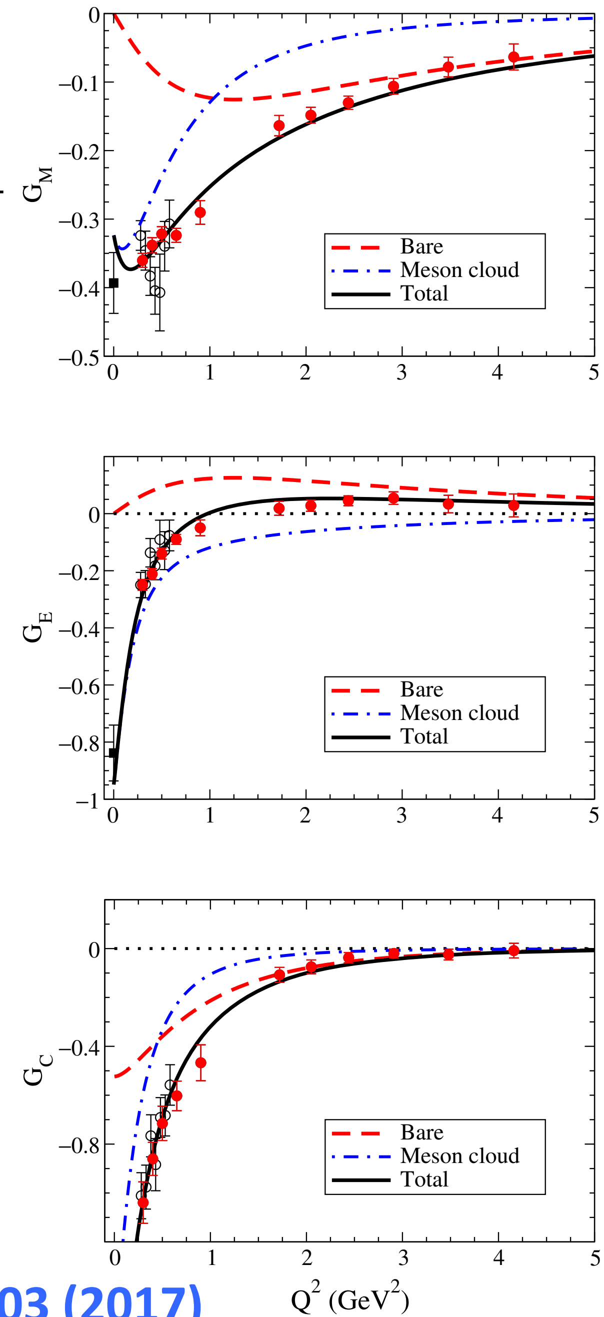

G. Ramalho, M. T. P. , PHYSICAL REVIEW D 95 014003 (2017)

$N \rightarrow N^*(1535)$ TFFs

$J^P = 1/2^-$ I=3/2
~50% decay to πN
~50% decay to ηN

$$J^\mu = \bar{u}_R \left[F_1^* \left(\gamma^\mu - \frac{\not{q} q^\mu}{q^2} \right) + F_2^* \frac{i\sigma^{\mu\nu} q_\nu}{M_N + M_R} \right] \gamma_5 u_N$$

- Use CST quark model to infer meson cloud from the data.

Again good agreement of bare quark core with EBAC analysis.

- Bare quark effects dominate F_1^* for large Q^2
- Meson cloud effects dominate F_2^* with meson cloud extending to high Q^2 region.

(effect from the ηN channel?).

$A^V_{1/2}(0) = 0.090 \pm 0.013$ GeV$^{-1/2}$ $A^S_{1/2}(0) = 0.015 \pm 0.013$ GeV$^{-1/2}$

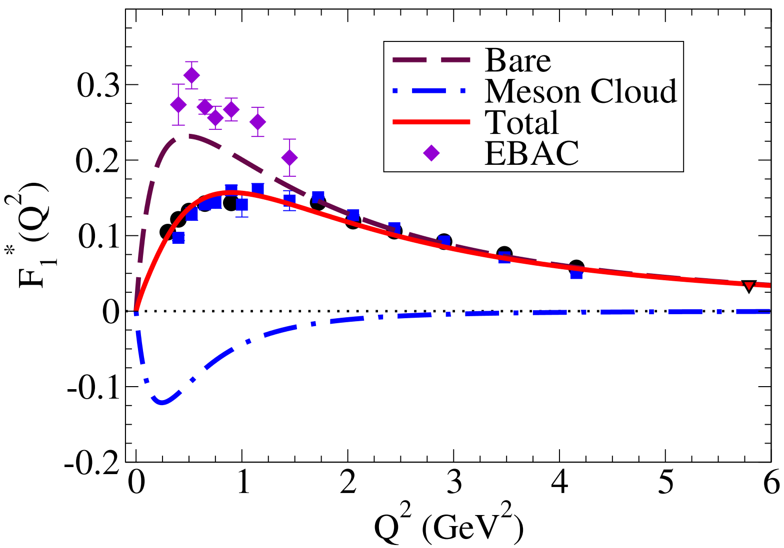

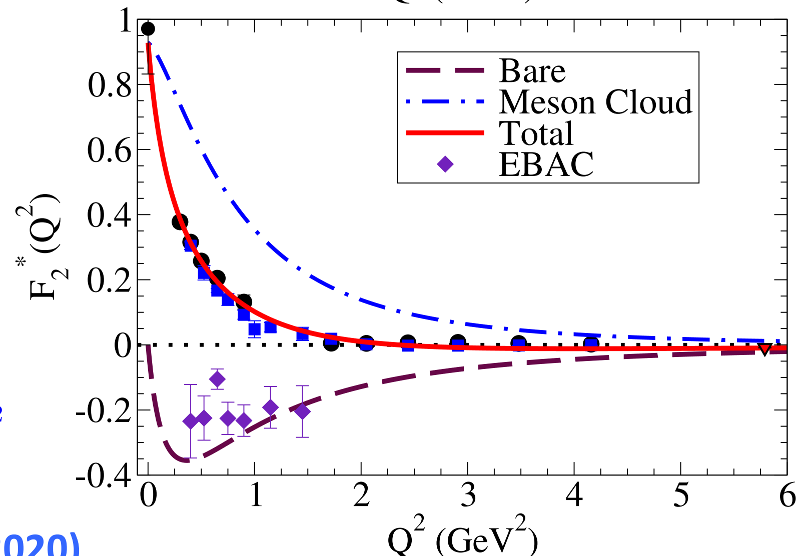

G. Ramalho, M. T. P. , PHYSICAL REVIEW D 101 114008 (2020)

Extension to the Timelike region

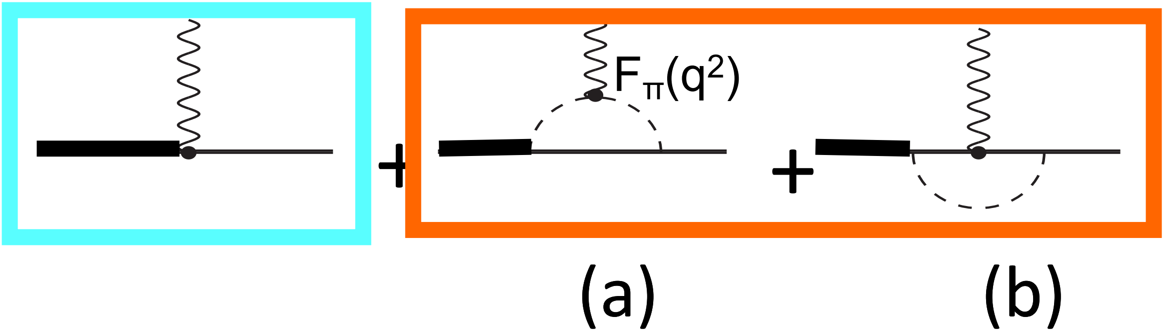

The residue of the pion from factor $F_\pi(q^2)$ at the timelike ρ pole is proportional to the $\rho \longrightarrow \pi\pi$ decay

Diagram (a) related with pion electromagnetic form factor $F_\pi(q^2)$

Crossing the boundaries

$\Delta(1232)$ Dalitz decay

Ramalho, Pena, Weil, Van Hees, Mosel, Phys.Rev. C93 (2016)

$\gamma N \rightarrow \Delta$

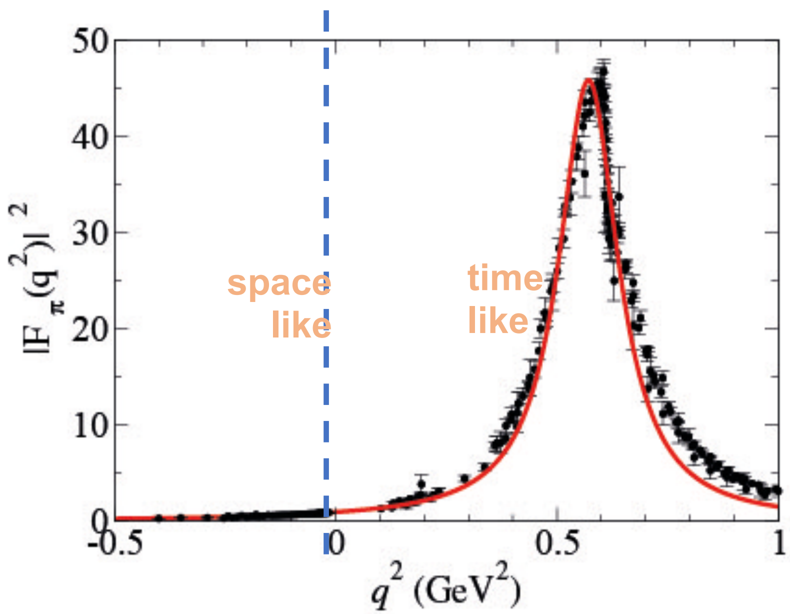

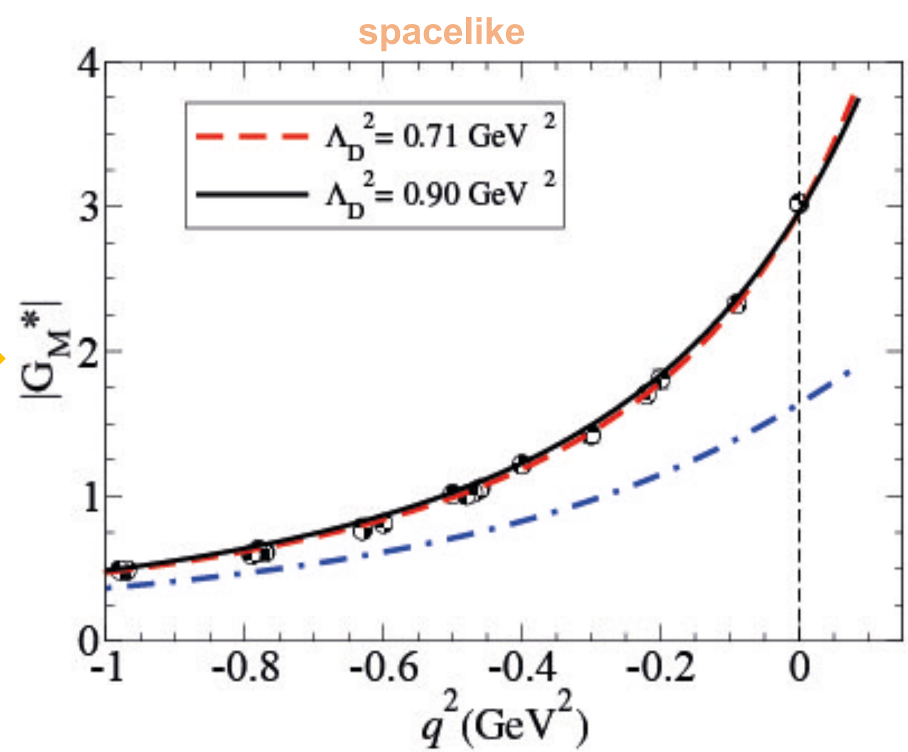

Parametrization of pion Form Factor

$$F_\pi(q^2) = \frac{\alpha}{\alpha - q^2 - \frac{1}{\pi}\beta q^2 \log\frac{q^2}{m_\pi^2} + i\beta q^2}$$

$\alpha = 0.696$ GeV^2

$\beta = 0.178$

Timelike region

$\Delta(1232)$ Dalitz decay

$$\Gamma_{\gamma^* N}(q;W) = \frac{\alpha}{16}\frac{(W+M)^2}{M^2W^3}\sqrt{y_+ y_-}\, y_- |G_T(q^2,W)|^2$$

$$|G_T(q^2;M_\Delta)|^2 = |G_M^*(q^2;W)|^2 + 3|G_E^*(q^2;W)|^2 + \frac{q^2}{2W^2}|G_C^*(q^2;W)|^2$$

$$y_\pm = (W \pm M)^2 - q^2$$

$$\Gamma_{\gamma N}(W) \equiv \Gamma_{\gamma^* N}(0;W)$$

$$\Gamma_{e^+e^- N}(W) = \frac{2\alpha}{3\pi}\int_{2m_e}^{W-M} \Gamma_{\gamma^* N}(q;W)\frac{dq}{q}$$

Radiative decay widths

N*(1520) $J^P=3/2^-$ $I=1/2$
60% decay πN
30% decay to $\pi\Delta$

Proton

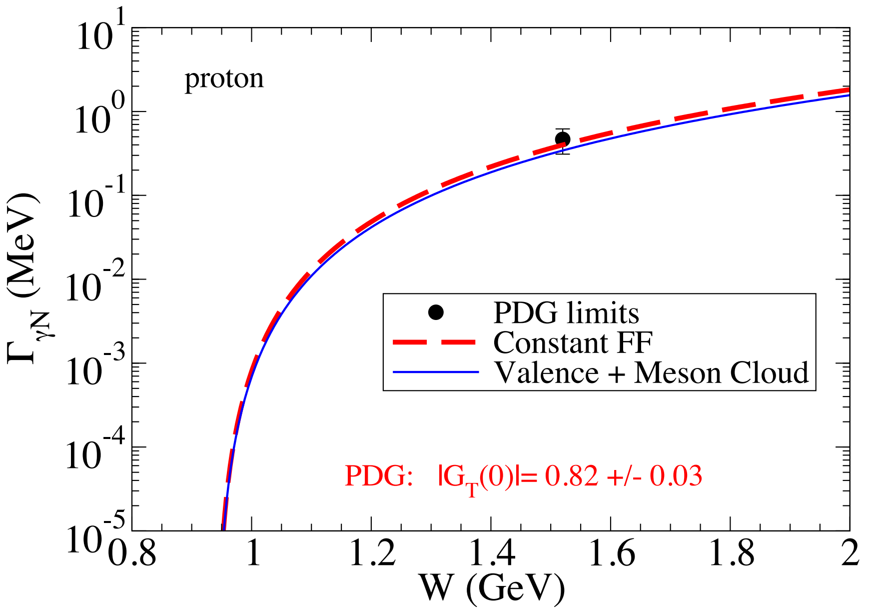

Neutron

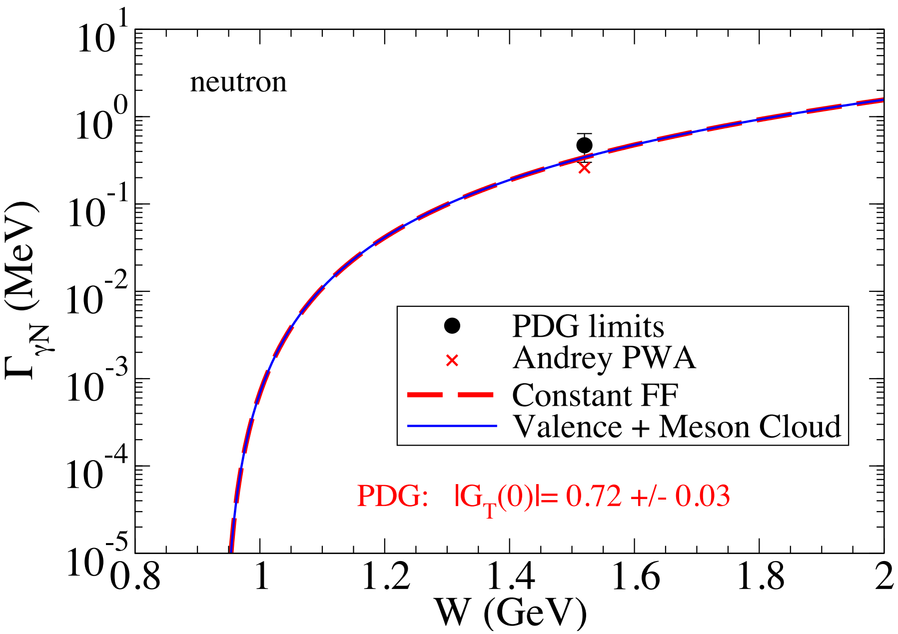

G. Ramalho and M.T. P. Phys. Rev. D 95, 014003 (2017)

Devenish (1976) normalization of transition form factors

Result Consistent with PDG value for γN decay width.

Dielectron Dalitz decay widths N*(1520)

Neutron and Proton light dilepton decay width

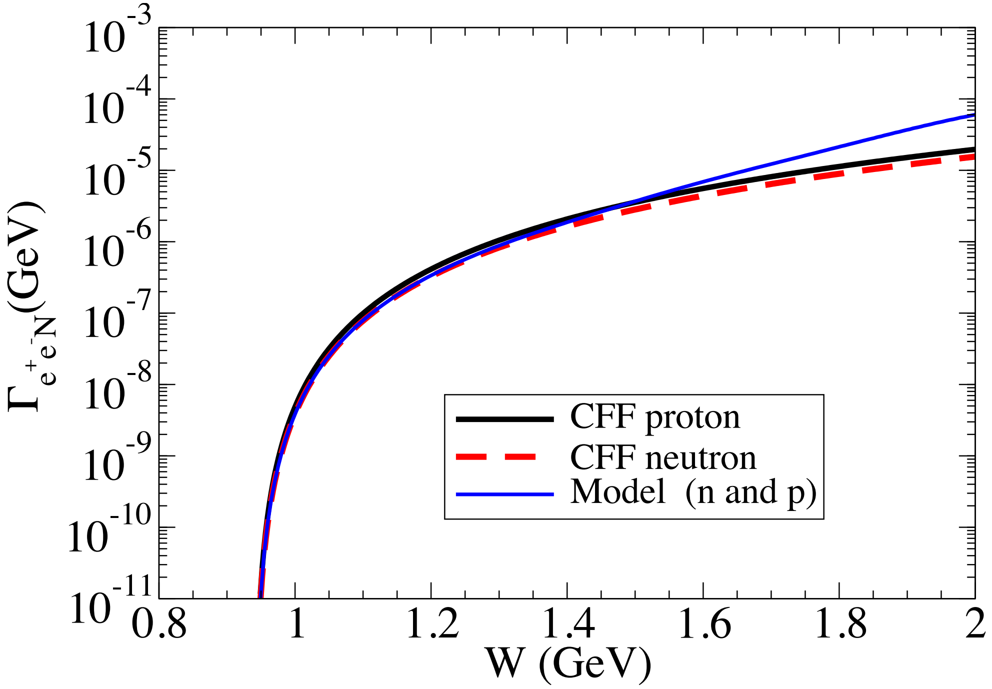

G. Ramalho and M.T. P. Phys. Rev. D 95, 014003 (2017)

Similar Proton and neutron results due to iso-vector dominance of meson cloud.

At higher energies evolution of $G_T(q^2, W)$ with q^2 becomes important.

Decay widths

N*(1535) $J^P=1/2^-$ I=1/2
~50% decay to π N
~50% decay to η N

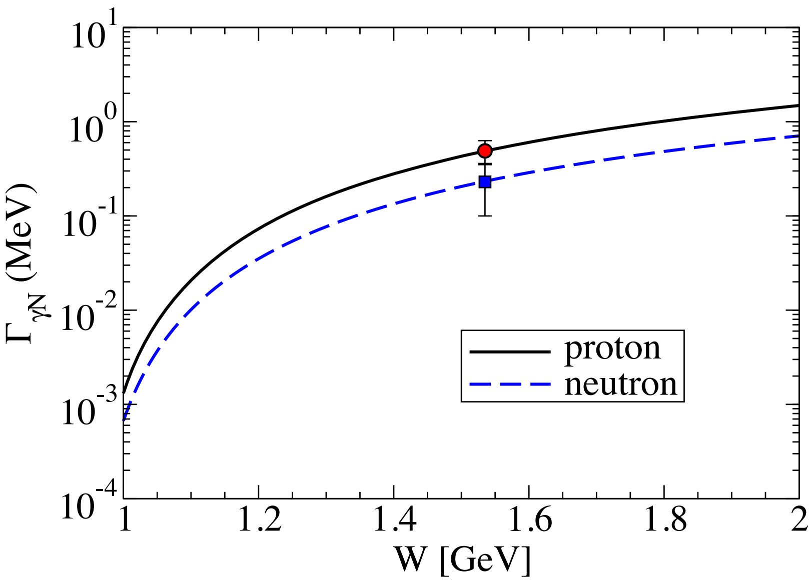

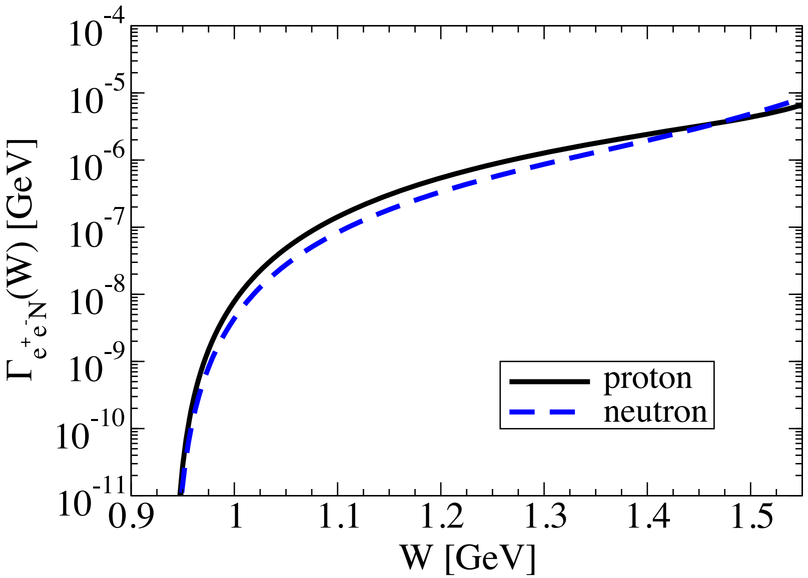

G. Ramalho and M.T. P. Phys.Rev.D 101 (2020) 11, 114008, (2020)

Different results for proton and neutron electromagnetic widths due to iso-scalar term in the eta meson cloud.

Timelike results give information on the neutron.

	$A_{1/2}(0)$ [GeV$^{-1/2}$]		$\Gamma_{\gamma N}$ [MeV]		
	Data	Model	Estimate	PDG limits	Model
p	0.105 ± 0.015	0.101	0.49 ± 0.14	0.19–0.53	0.503
n	-0.075 ± 0.020	-0.074	0.25 ± 0.13	0.013–0.44	0.240

Comparison between different resonances

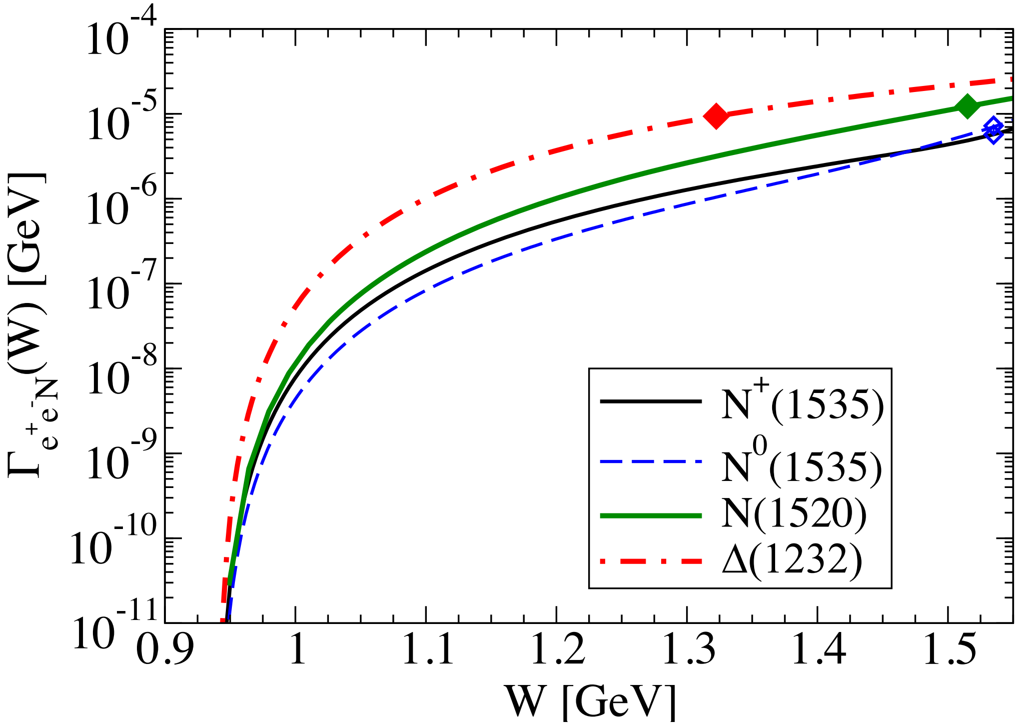

G. Ramalho and M.T. P. Phys.Rev.D 101 (2020) 11, 114008, (2020)

Dominance of the J=3/2 channel

Dilepton mass spectrum $\Delta(1232)$ Dalitz decay

HADES Collaboration, Phys.Rev. C95 0652205 (2017)

proton-proton collisions @1.25 GeV

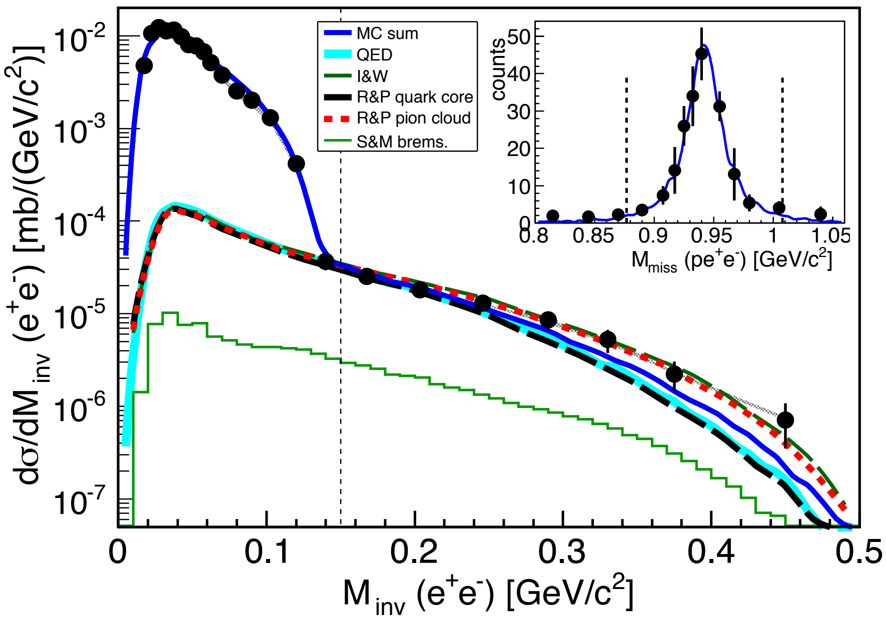

Signature of form factors q^2 dependence

Δ Dalitz decay branching ratio extracted 4.19 x 10^{-5}

$\Gamma(pe^+e^-)/\Gamma_{total}$ Γ_5/Γ

VALUE (units 10^{-5})	*DOCUMENT ID*
4.19±0.34±0.62	[1] ADAMCZEW... 17

[1] The systematic uncertainty includes the model dependence.

Entry in PDG

The obtained Δ Dalitz branching ratio at the pole position is equal to 4.19×10^{-5} when extrapolated with the help of the Ramalho-Peña model [27], which is taken as the reference, since it describes the data better. The branching ratio

Dilepton mass spectrum

N*(1520) + N*(1535)
Dalitz decay

True CST prediction: Red line

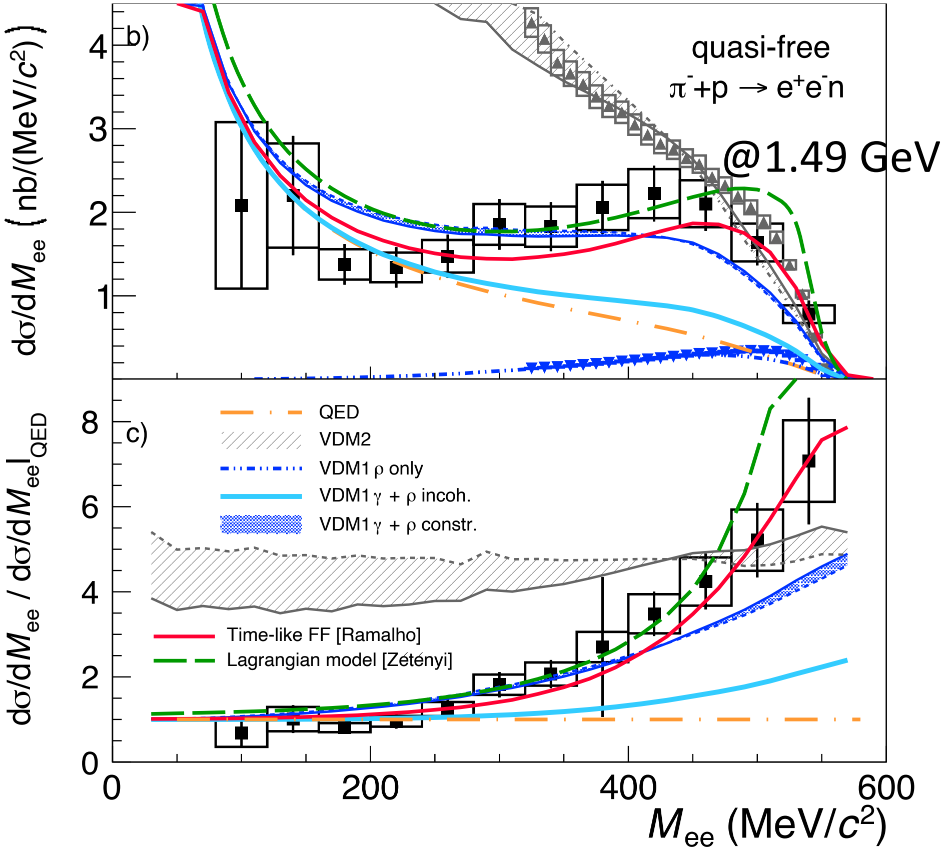

Simulations based on the CST model (**red line**) for these resonances also give a satisfactory description of the data.

Below 200 MeV/c2 , data agrees with a pointlike baryon-photon vertex (QED orange line) .

At larger invariant masses, data is more than 5 times larger than the pointlike result, showing a strong effect of the transition form factor.

HADES Collaboration
"First measurement of massive virtual photon emission from N* baryon resonances" e-Print: 2205.15914 [nucl-ex]

Extension to Strangeness in the timelike region

CST seems to work well at large Q^2.

$$e^+e^- \to \gamma^* \to B\bar{B}$$

$$|G(q^2)|^2 = \left(1+\frac{1}{2\tau}\right)^{-1}\left[|G_M(q^2)|^2 + \frac{1}{2\tau}|G_E(q^2)|^2\right.$$
$$= \frac{2\tau|G_M(q^2)|^2 + |G_E(q^2)|^2}{2\tau+1}. \quad \tau = \frac{q^2}{4M_B^2}$$

Effective Form factor that gives the integrated cross section

Unitarity and Analiticity demand that for $q^2 \to \infty$

$$G_M(q^2) \simeq G_M^{\mathrm{SL}}(-q^2),$$
$$G_E(q^2) \simeq G_E^{\mathrm{SL}}(-q^2).$$

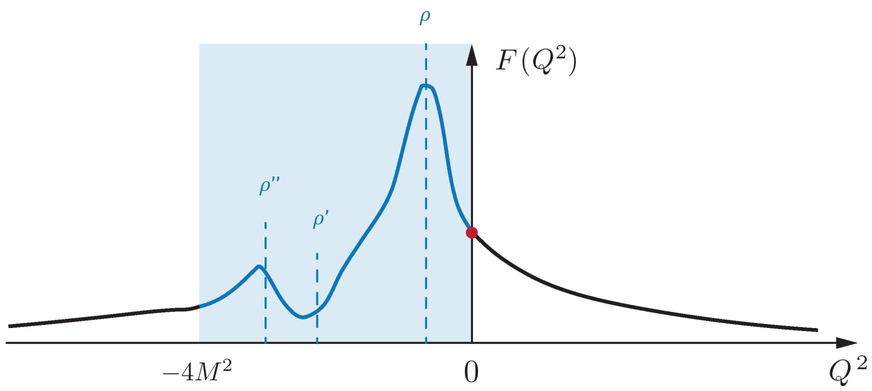

S.Pacetti, R. Baldini Ferroli and E. Tomasi-Gustafsson, Phys. Rept. 550-551,1 (2015)

Extension to Strangeness in the timelike region

$$e^+e^- \to \gamma^* \to B\bar{B}$$

Data from
Babar,CLEO,BESIII

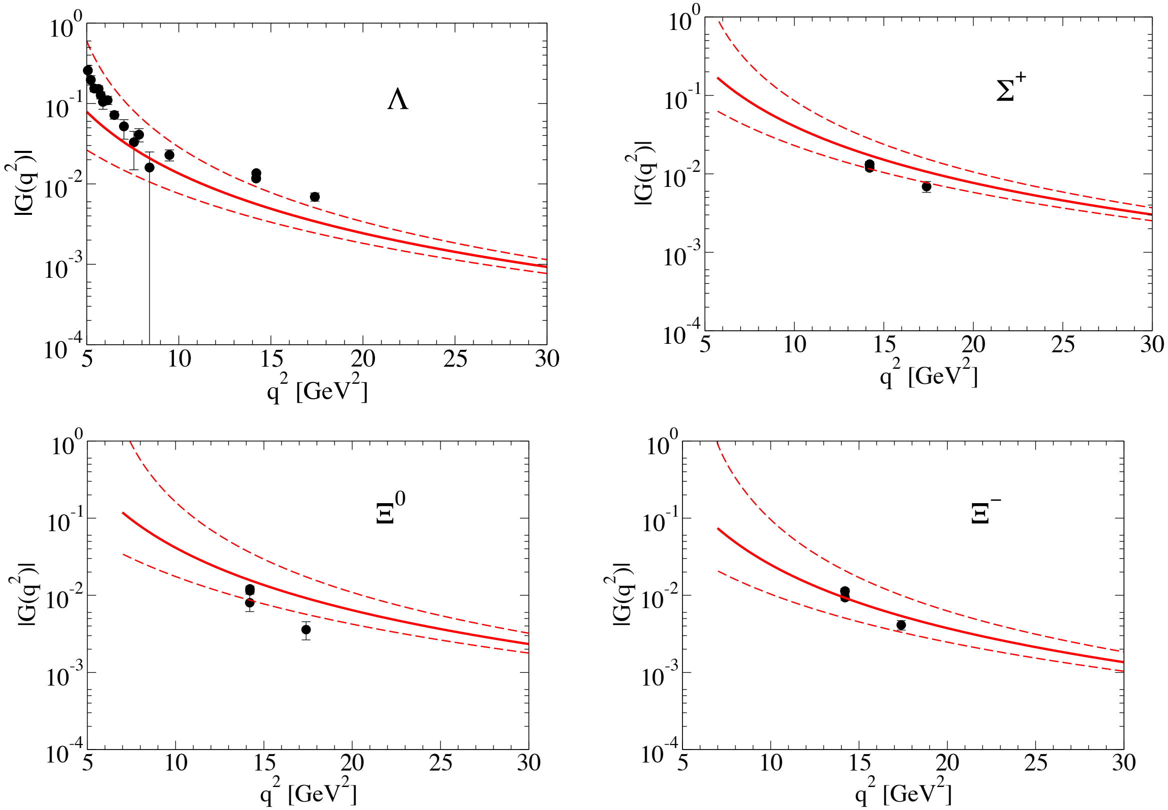

Full line: $G(q^2) = G(2M^2 - q^2)$

Dashed lines: $G(q^2) = G(4M^2 - q^2)$

$$G(q^2) = G(-q^2)$$

$$G_M(q^2) \simeq G_M^{\rm SL}(-q^2),$$
$$G_E(q^2) \simeq G_E^{\rm SL}(-q^2).$$

G. Ramalho and M.T.P. Phys.Rev.D 101 (2020) 1, 014014, (2020)

Asymptotic behavior reached at energies higher than reflection property

$$e^+e^- \to \gamma^* \to B\bar{B}$$

Perturbative QCD limit is way above the region where refletion symmetry starts to be valid **(100 GeV² versus 10 GeV²)**

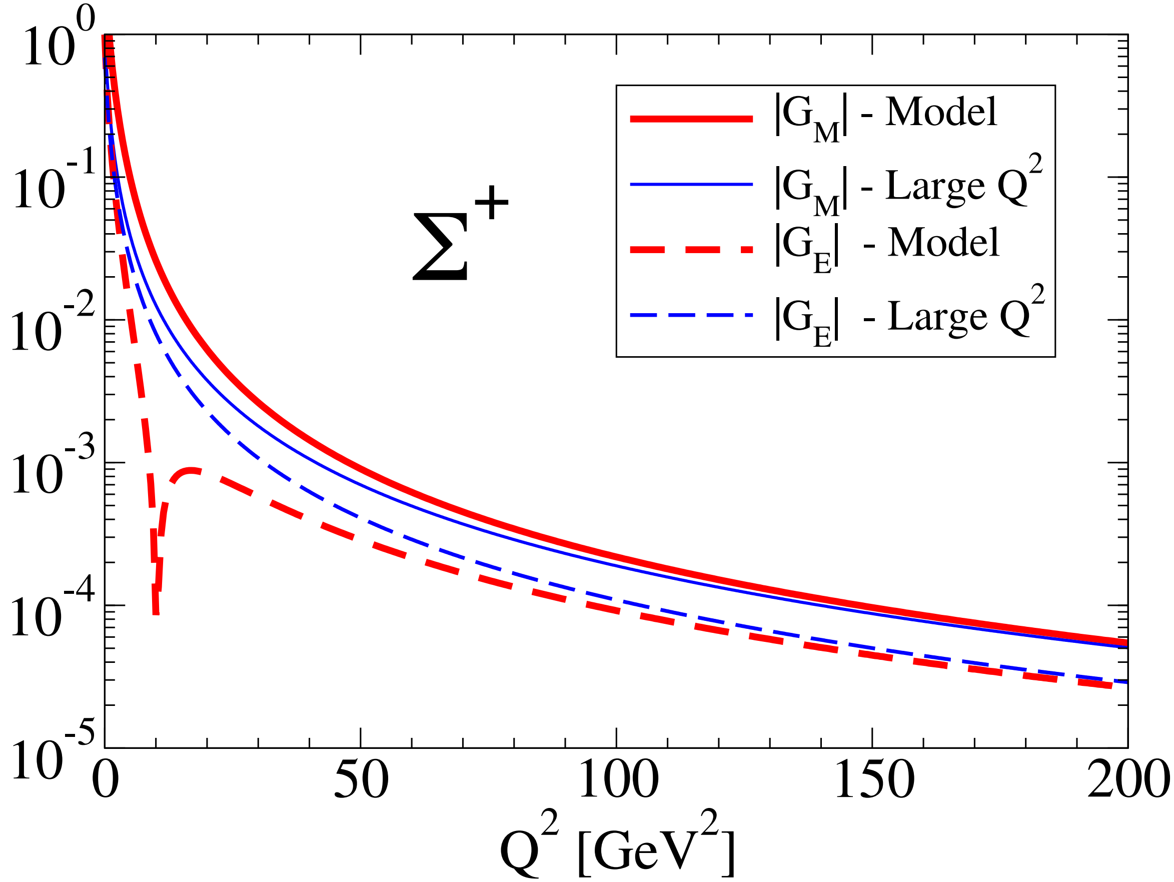

Summary

With a CST phenomenological ansatz for the baryon wave functions we described different excited states of the nucleon, with a variety of spin and orbital motion.

1 Evidence of separation of partonic and hadronic (pion cloud) effects from the Δ (1232)

2 Made consistent with LQCD in the large pion mass regime, enabling extraction of "pion cloud" effects indirectly from data.

3 Spacelike e.m. transition FFs for:
N*(1440), N*(1520), N*(1535), ..., baryon octet, etc.

4 Extension to timelike e.m. transition FFs and predictions for dilepton mass spectrum and decay widths.

5 Descriptions consistent with experimental data at high Q^2.

Back up slides

Crossing the Boundaries to explore baryon resonances

$$Q^2 = -q^2$$

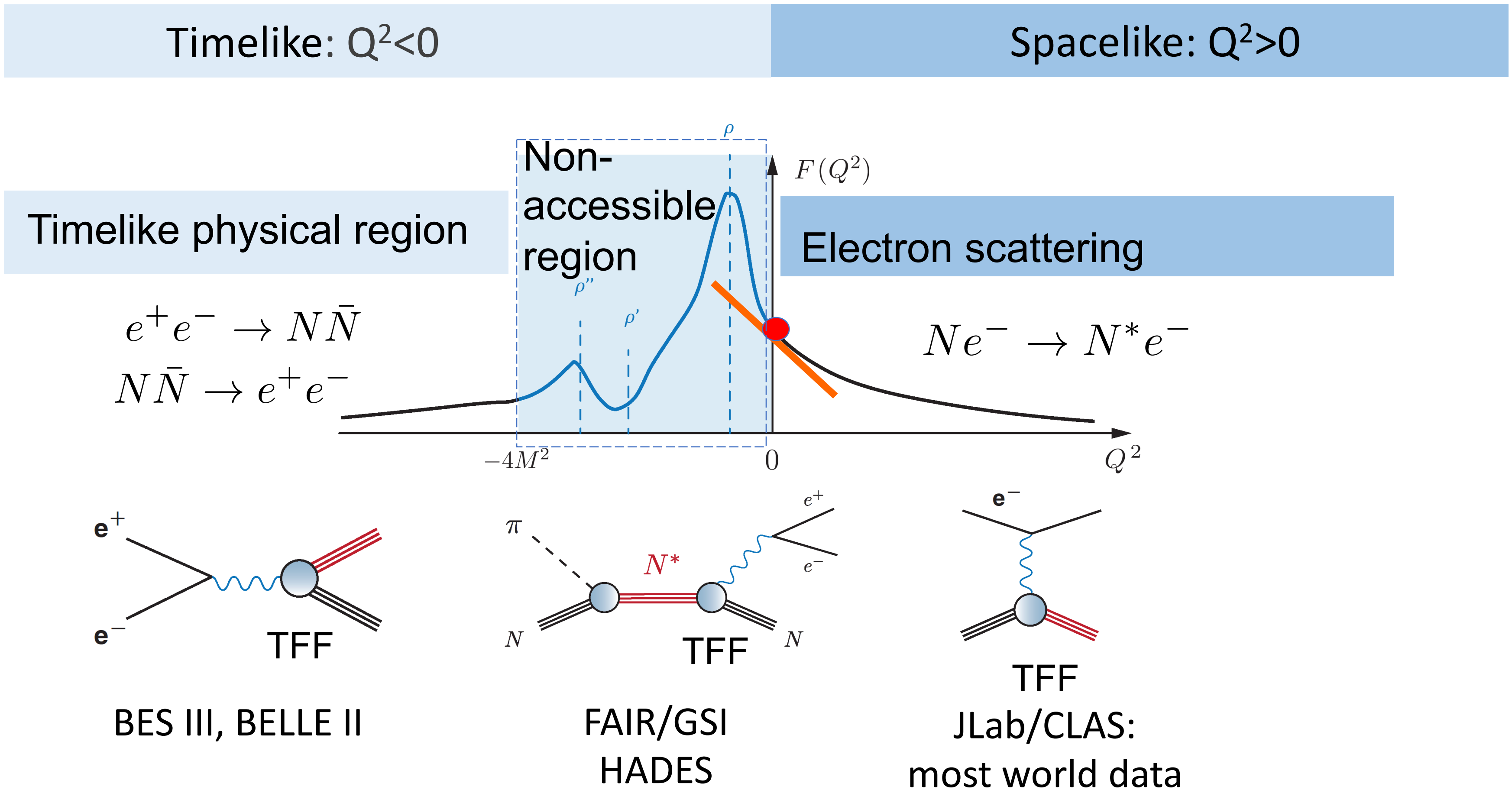

Results have to match at the photon point.

CLAS/JLab electron scattering data constrain interpretation of dilepton production data.

CST© Covariant Spectator Theory

- Formulation in Minkowski space.

- Motivation is partial cancellation

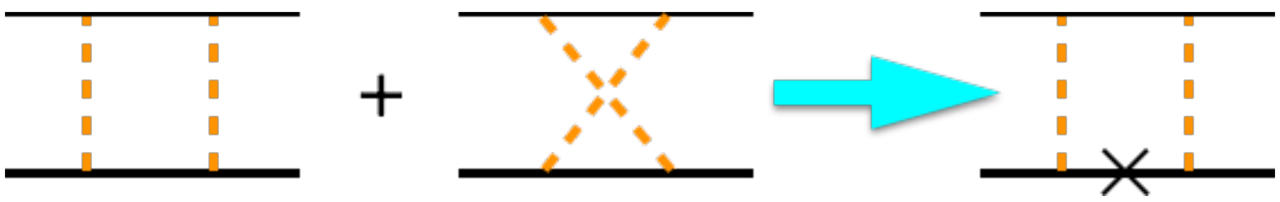

- Manifestly covariant, although only three-dimensional loop integrations.

$$\int_k = \int \frac{d^3\mathbf{k}}{2E_D(2\pi)^3}$$

- Provides wave functions from covariant vertex with simple transformation properties under Lorentz boosts, appropriate angular momentum structures and smooth non-relativistic limit.

$$f(Q^2) = e + gB(Q^2)e + gB(Q^2)gB(Q^2)e + \cdots = e + \frac{gB(Q^2)e}{1 - gB(Q^2)}$$

if $gB(Q^2) = \frac{\lambda^2}{\Lambda^2 + Q^2}$, then $f(Q^2) = e + \frac{\lambda^2 e}{\Lambda^2 - \lambda^2 + Q^2}$

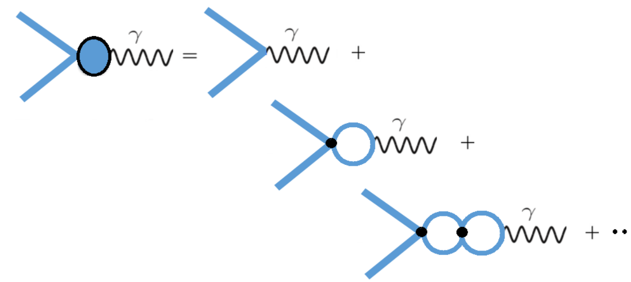

$$f_{1\pm} = \lambda + \frac{1-\lambda}{1 + Q_0^2/m_v^2} + \frac{c_\pm Q_0^2/M_h^2}{\left(1 + Q_0^2/M_h^2\right)^2}$$

$$f_{2\pm} = \kappa_\pm \left(\frac{d_\pm}{1 + Q_0^2/m_v^2} + \frac{(1 - d_\pm)}{1 + Q_0^2/M_h^2} \right)$$

$$\Gamma_\mu(p,Q) = \gamma_\mu + \int \frac{d^4q}{(2\pi)^4} K(p,q,Q) S(q+\eta Q) \Gamma_\mu(q,Q) S(q-\eta Q)$$

To parametrize the current use Vector Meson Dominance at the quark level
a truncation to the rho and omega poles of the full meson spectrum
contribution to the quark-photon coupling.

4 parameters

$\gamma N \rightarrow \Delta$

Connection to Lattice QCD

To control model dependence:

CST model and LQCD data are made **compatible.**

G. Ramalho and M. T. Peña, Phys. Rev. D 80, 013008 (2009)

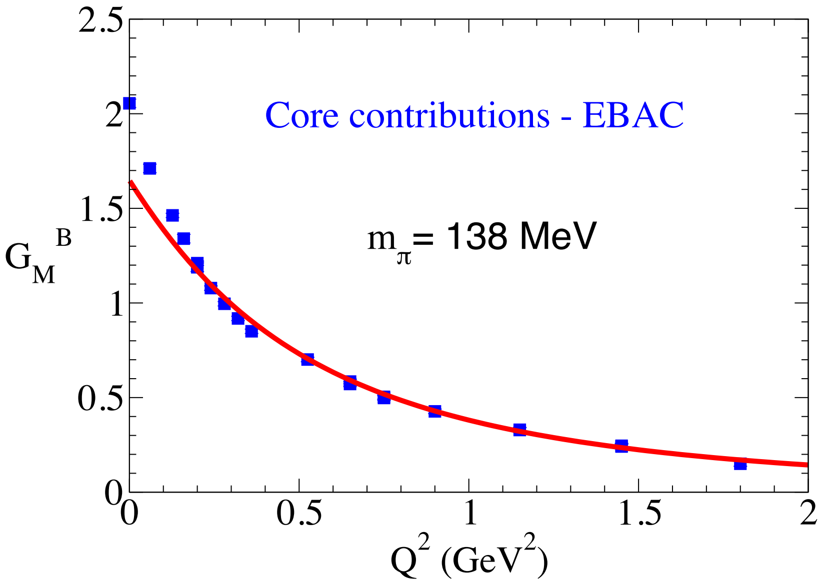

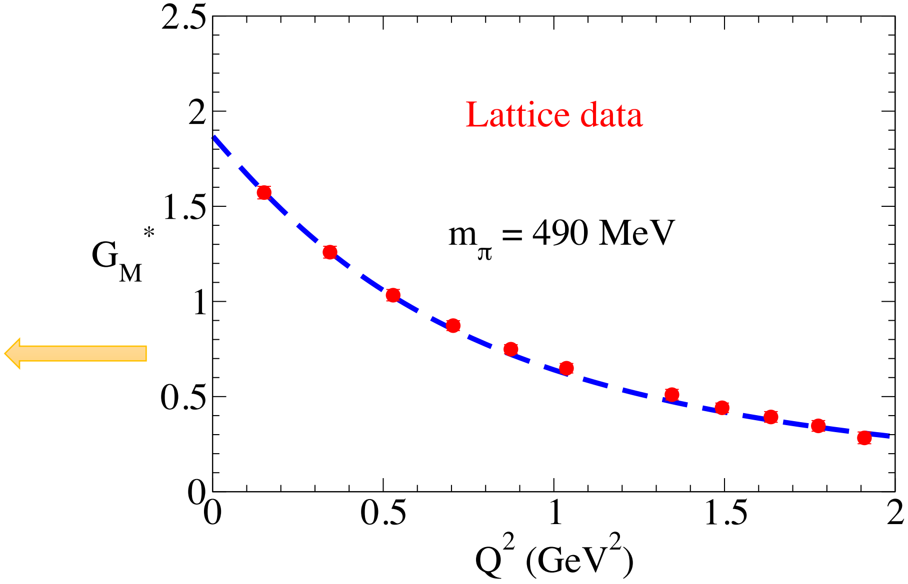

Model (no pion cloud) valid for lattice pion mass regime.
No refit of wave function scale parameters for the physical pion mass limit.

$N \to N^*(1520)$

PDG data at the photon point:

	$A_{1/2}$	$A_{3/2}$	$\|A\|^2$
p	-0.025 ± 0.005	0.140 ± 0.005	20.2 ± 1.4
n	-0.050 ± 0.005	-0.120 ± 0.005	15.7 ± 1.3

$$A^V_{3/2} \approx 0.13 \; ; A^S_{3/2} \approx 0.01 \, (GeV^{-1/2})$$

Dominance of iso-vector channel concurs to our model of the meson cloud: pion only

$N \to N^*(1535)$

Iso-vector + iso-scalar channels included into our model of the meson cloud: pion and eta cloud.

$$F_1^{\rm MC} = Q^2 \tilde{C}(Q^2)\tau_3 \qquad F_2^{\rm MC} = A(Q^2) + B(Q^2)\tau_3$$

PDG data at the photon point:

$$A^V_{1/2}(0) = 0.090 \pm 0.013 \text{ GeV}^{-1/2}$$
$$A^S_{1/2}(0) = 0.015 \pm 0.013 \text{ GeV}^{-1/2}$$

↓

Isovector dominance to some extent

Extension to Timelike

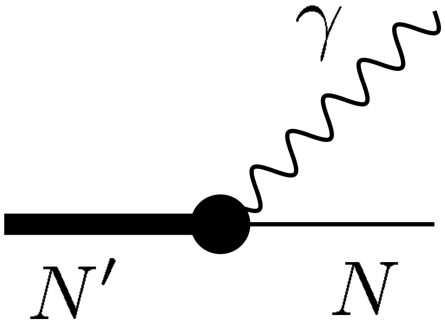

R rest frame

$$P_R = (W, 0, 0, 0); \quad P_N = (E_N, 0, 0, -|\mathbf{q}|); \quad q = (\omega, 0, 0, |\mathbf{q}|)$$

Timelike $q^2 > 0$

$$\omega = \frac{W^2 - M^2 + q^2}{2W}$$

$$|\mathbf{q}|^2 = \frac{[(W+M) - q^2][(W-M)^2 - q^2]}{4W^2}$$

$$E_N = \frac{W^2 + M^2 - q^2}{2W}$$

Spacelike $-q^2 = Q^2 > 0$

$$\omega = \frac{W^2 - M^2 - Q^2}{2W}$$

$$|\mathbf{q}|^2 = \frac{[(W+M) + Q^2][(W-M)^2 + Q^2]}{4W^2}$$

$$E_N = \frac{W^2 + M^2 + Q^2}{2W}$$

TL: $q^2 \leq (W - M)^2$ $\qquad$ $W \geq M$

Transition form factors in the timelike region are restricted to a given kinematic region that depends on the varying resonance mass W.

Extension to Timelike

$$\gamma N \rightarrow \Delta$$

- Extension to higher W shows effect of the rho mass pole
- In that pole region small bare quark contribution (thin lines)

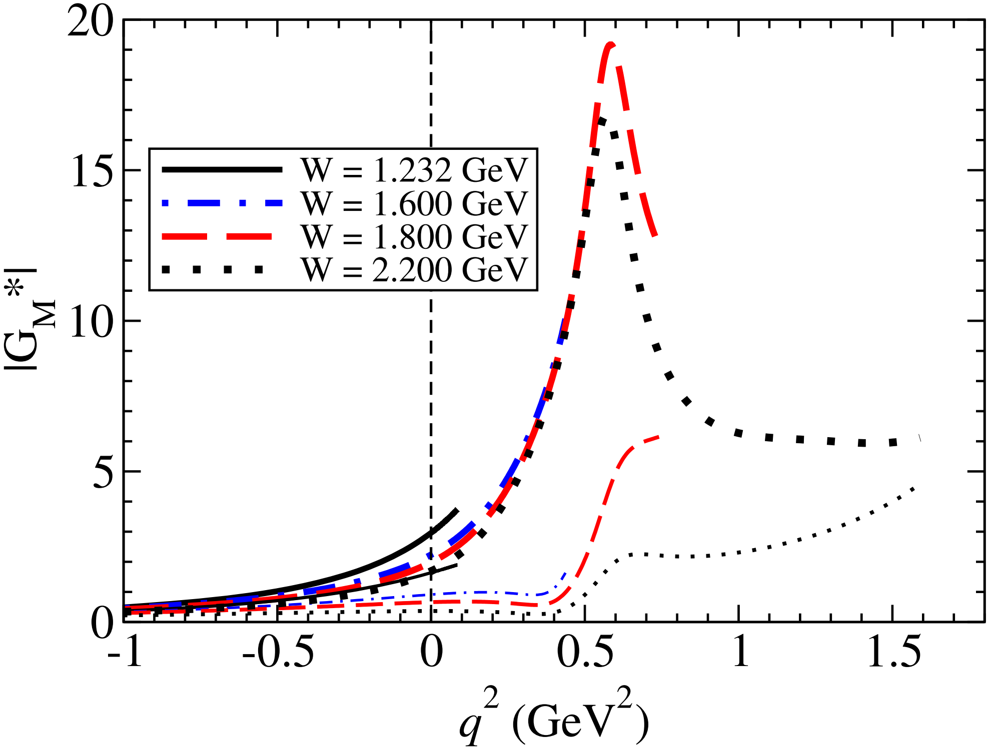

Crossing the boundaries

N*(1520) Dalitz decay

True prediction

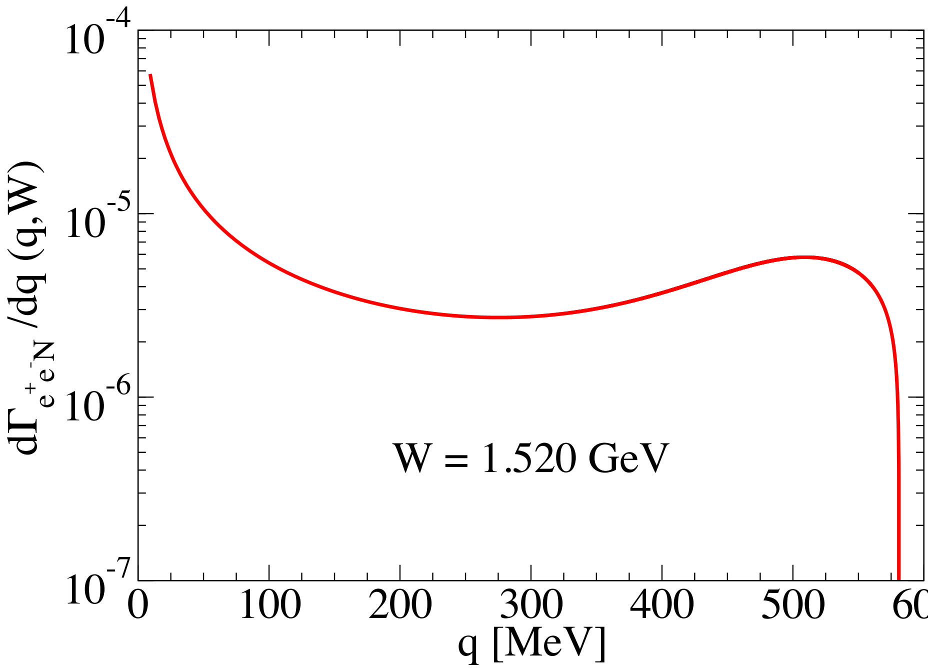

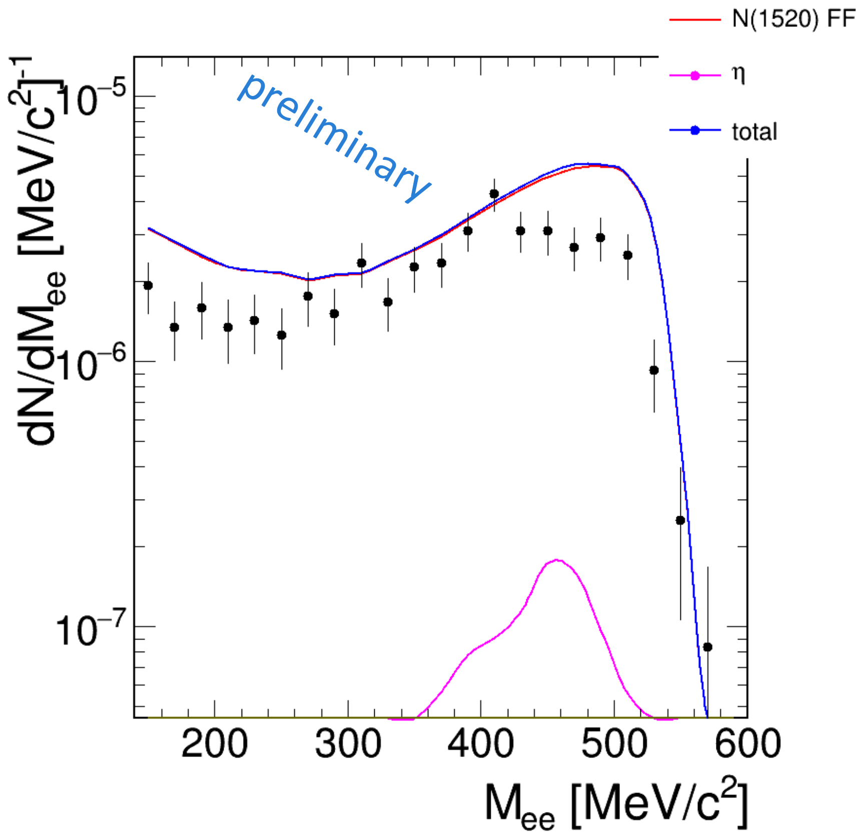

HADES Collaboration
2018

Crossing the boundaries

$N^*(1520)$ Dalitz decay

Effect of dependence of e.m. coupling with W   True prediction

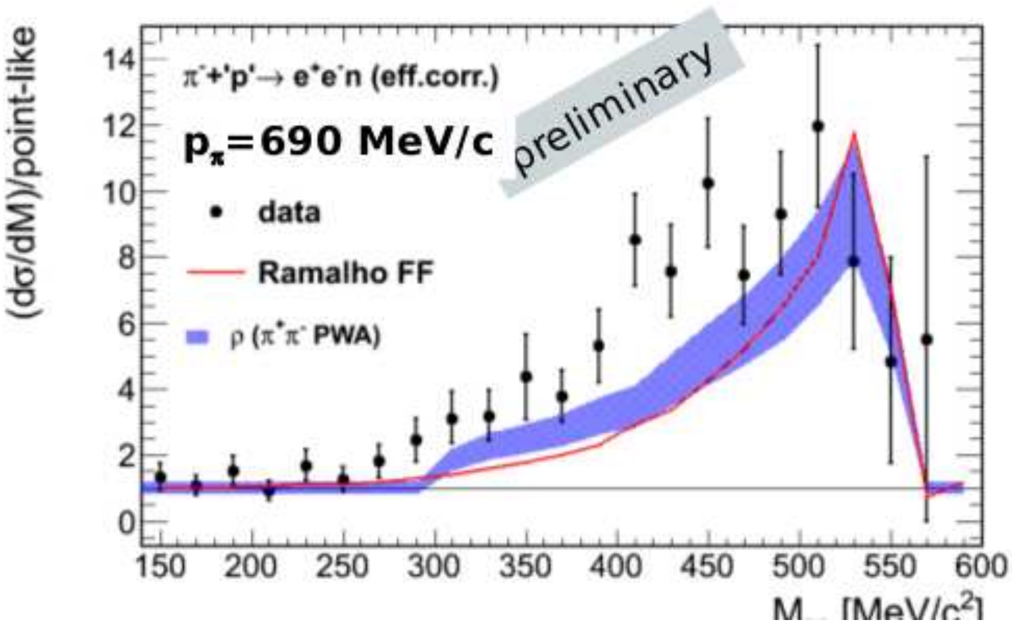

B. Ramstein, NSTAR2019   HADES Collaboration

Ratio to pointlike case

Crossing the boundaries

N*(1535) Dalitz decay

$$\Gamma_{\gamma^* N}(q,W) = \frac{\alpha}{2W^3}\sqrt{y_+ y_-}\, y_+ B \| G_T(q^2,W)|^2,$$

$$|G_T(q^2,W)|^2 = |G_E(q^2,W)|^2 + \frac{q^2}{2W^2}|G_C(q^2,W)|^2$$

$$\frac{d\Gamma_{e^+e^-N}}{dq}(q,W) = \frac{2\alpha}{3\pi q^3}(2\mu^2+q^2)\sqrt{1-\frac{4\mu^2}{q^2}}\,\Gamma_{\gamma^* N}(q,W),$$

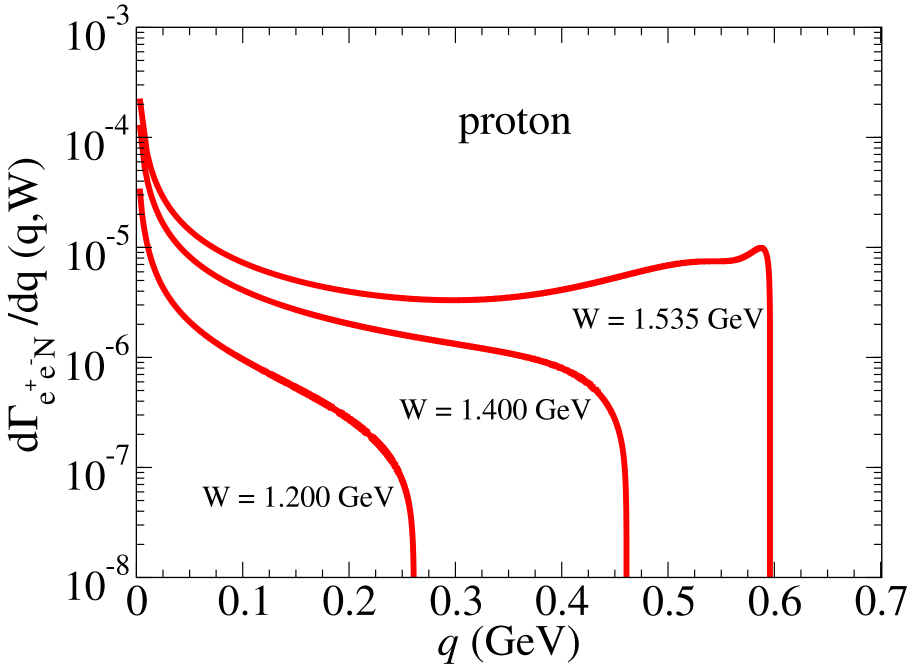

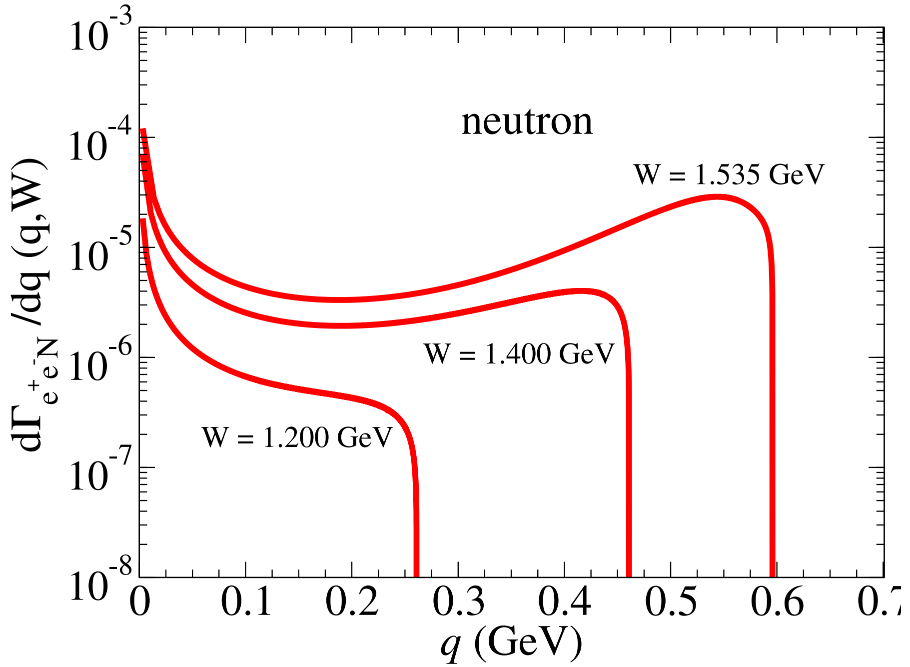

Extension to Strangeness in the Spacelike region with a global fit to lattice data and physical magnetic moments

Extend the parametrization of the e.m. current to the valence quark d.o.f of the **whole** baryon octet.

$$j_i = \frac{1}{6} f_{i+} \lambda_0 + \frac{1}{2} f_{i-} \lambda_3 + \frac{1}{6} f_{i0} \lambda_s$$

$$\lambda_0 = \begin{pmatrix} 1 & 0 & 0 \\ 0 & 1 & 0 \\ 0 & 0 & 0 \end{pmatrix}, \qquad \lambda_3 = \begin{pmatrix} 1 & 0 & 0 \\ 0 & -1 & 0 \\ 0 & 0 & 0 \end{pmatrix}$$

$$\lambda_s \equiv \begin{pmatrix} 0 & 0 & 0 \\ 0 & 0 & 0 \\ 0 & 0 & -2 \end{pmatrix}$$

Parameters for valence quark degrees of freedom and the pion cloud dressing determined by a **global fit** to octet baryon lattice data for the e.m. form factors and physical magnetic moments.

Two examples:

Red line: lattice
Blue line: physical regime

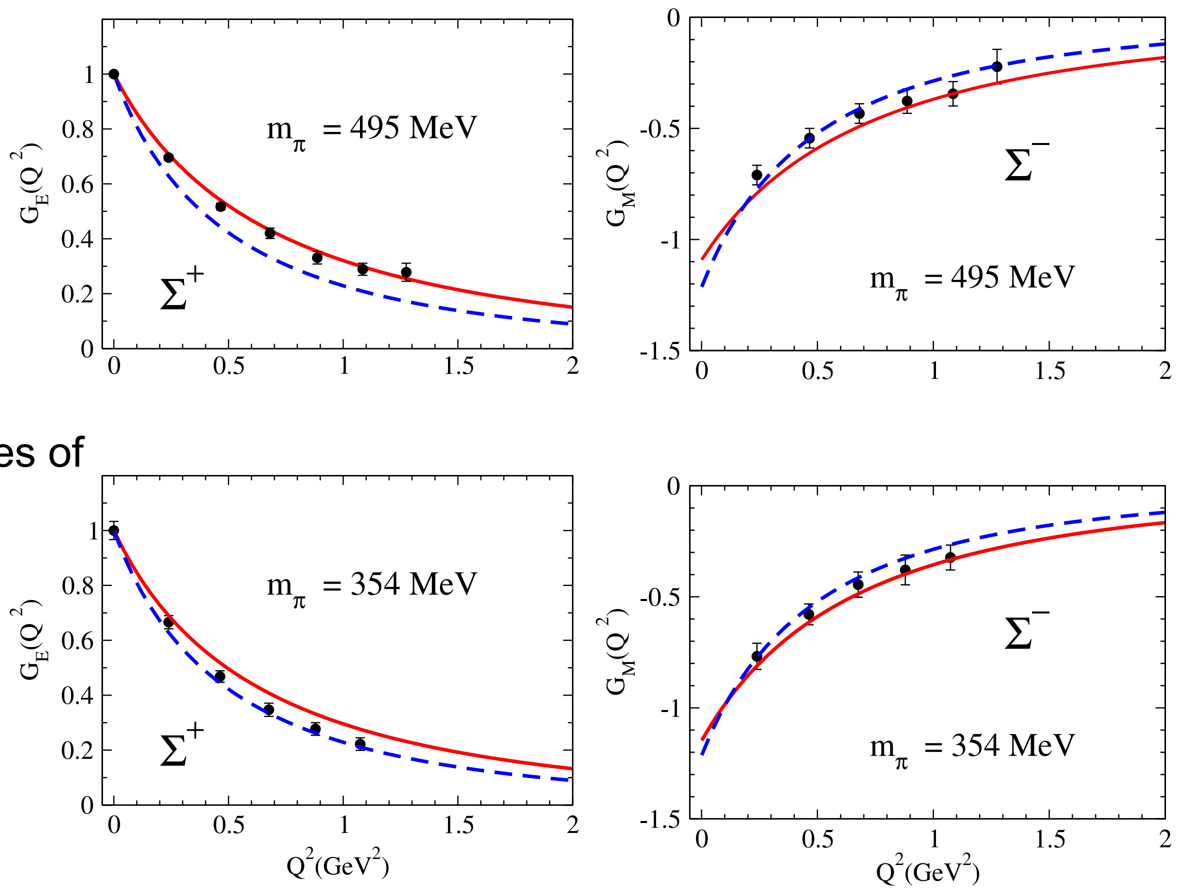

Lattice data:
H.W. Lin and K. Orginos, Phys. Rev. D 79, 074507 (2009).

G. Ramalho and K.Tsushima, PRD 84, 054014 (2011)

Asymptotic behavior

$e^+e^- \to \gamma^* \to B\bar{B}$

Perturbative QCD limit is way above the region where refletion symmetry starts to be valid

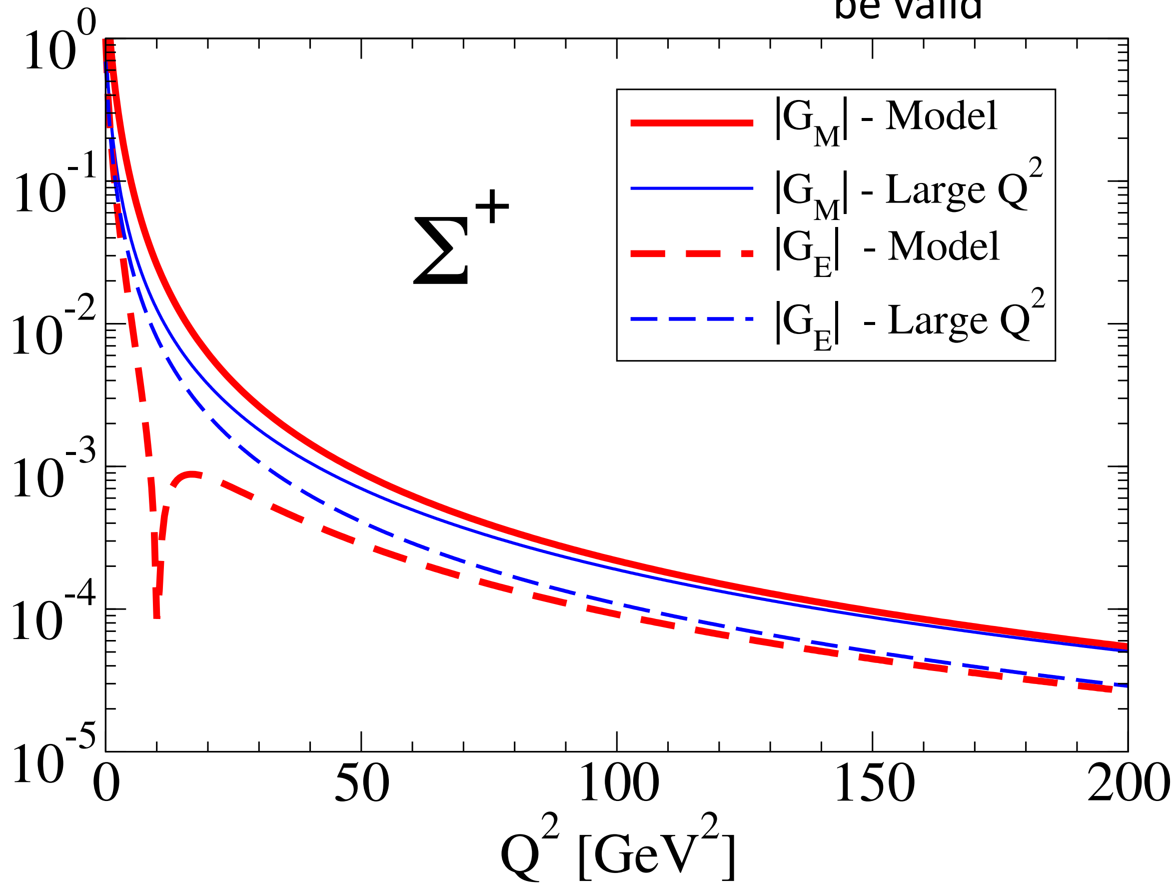

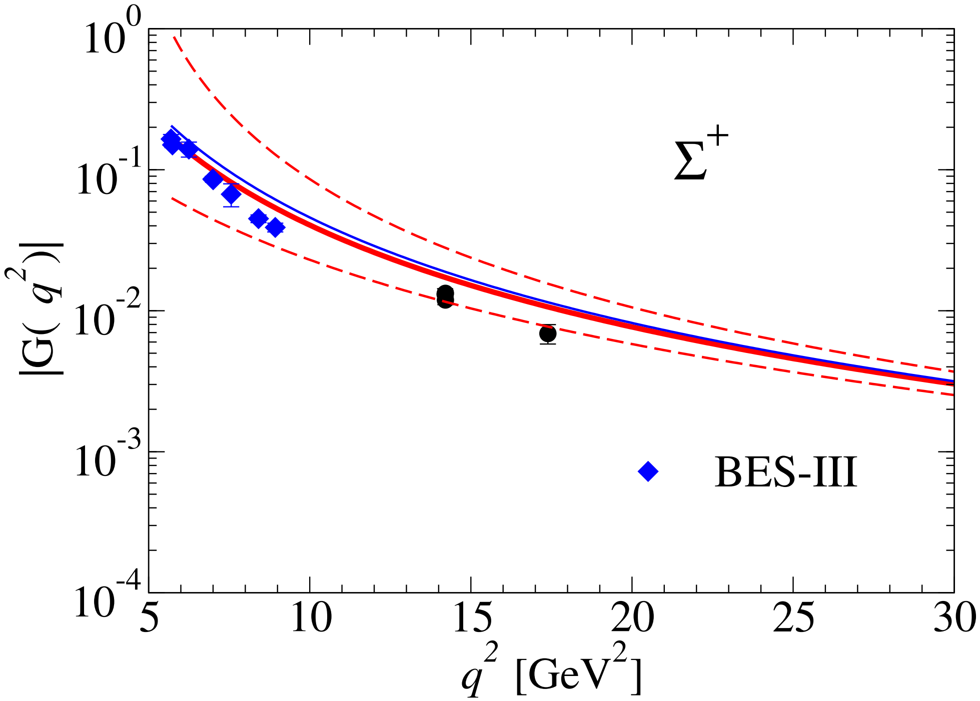

10^0
10^{-1}
10^{-2}
10^{-3}
10^{-4}
5
10
15
20
25
30
$|G(q^2)|$
q^2 [GeV^2]
Σ^+
BES-III

Predictive power:

D13(J=3/2-) S11(J=1/2-) (I=1/2) are part of a large supermultiplet (SU(6) spin-flavor with O(3) symmetry)

S. Capstick and W. Roberts, Prog. Part. Nucl. Phys. 45, S241 (2000);
V. D. Burkert et al. Phys. Rev. C 67, 035204 (2003).

Input: $N(1520), N(1535)$; **Output:** $N(1650), N(1700), \Delta(1620), \Delta(1700)$

D13 S11 S11 D13 S31 D33

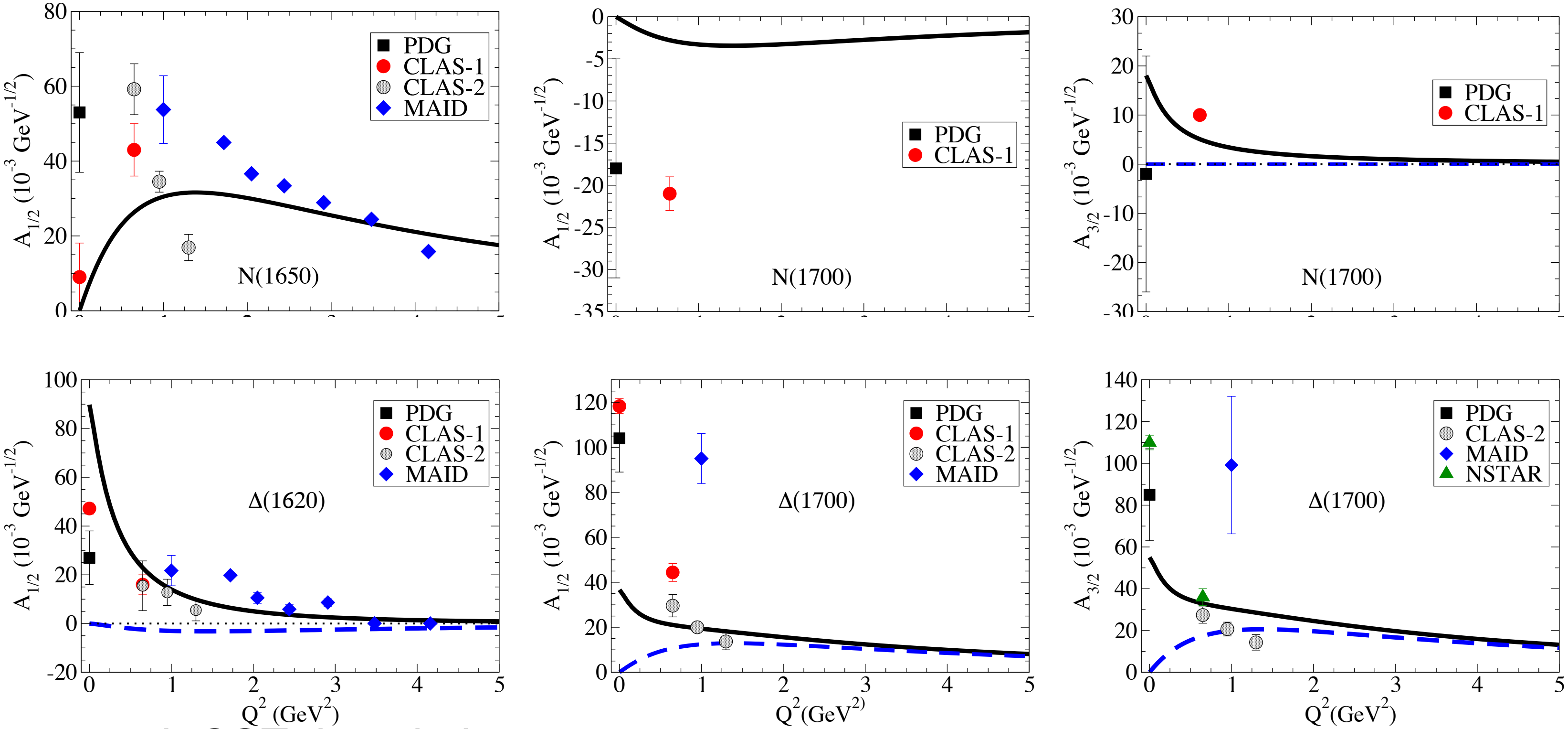

Bare quark CST description expected to work well in high Q^2 region!

G. Ramalho , PRD 90, 033010 (2014)

Summary

Covariant **S**pectator quark-diquark model for baryons enables description of different states, with a variety of spin and orbital motion.

Several applications: **Δ(1232)**, N*(1440), N*(1535)**, N*(1520),** DIS, dilepton mass spectrum, hyperons of the baryon octet.

Consistent with experimental data at high Q^2.

Made consistent with LQCD in the large pion mass regime informing on “pion cloud” effects, and **high q^2 behavior of time-like FFs**.

VMD and “pion cloud” sustained extension to the timelike region of the TFF of the **Δ(1232), N*(1520), N*(1535), ...**